Characterization of pre-gelatinized kidney bean (*Phaseolus vulgaris* L.) produced using microwave hot-air flow rolling drying technique

Mengge Li [a], Bo Wang [b], Weiqiao Lv [a,*], Rongru Lin [a], Donglin Zhao [c]

[a] *College of Engineering, China Agricultural University, Beijing, 100083, China*
[b] *School of Behavioural and Health Science, Australian Catholic University, Sydney, NSW, 2060, Australia*
[c] *The Center of Agro-processing, Chinese Academy of Agricultural Machanization Sciences, Beijing, 100083, China*

ARTICLE INFO

ABSTRACT

This study aims to develop a pretreatment and drying process for kidney beans to improve their cooking efficiency. Hot air drying (HD) and microwave hot air rolling drying (MHRD) were analyzed for the drying of pre-cooked kidney beans, and the effect of hot air and microwave on structure and gelatinization properties of kidney beans starch were investigated. The result indicated that the drying time was significantly reduced by approximately 27% ($p < 0.05$) with the increase of hot air temperature by 10 °C in the HD-processed material. Based on the incorporation of microwave radiation, drying time was further decreased by 2.5 times at the same hot air temperature. The microstructure, crystalline structure, thermal behavior and FTIR spectra of the kidney bean starch suggested the positive correlation between the hot air temperature/microwave radiation and destruction of their crystalline structure/gelatinization degree. The cooked dried kidney beans exhibited significantly decreased hardness, gumminess and chewiness and increased springiness, compared with the untreated kidney beans, suggesting an improved cooking efficiency. Base on the results of drying efficiency, color profile, gelatinization of kidney bean starch and texture profile analysis of the cooked beans, MHRD-70 was the optimum drying process.

1. Introduction

Kidney bean (*Phaseolus vulgaris* L.) is a member of the legume family (Qin et al., 2019). It is rich in a variety of macro- and micro-nutrients, including starch (Punia, Dhull, Sandhu, Kaur, & Purewal, 2020), protein (Ahmed, Al-Ruwaih, Mulla, & Rahman, 2018), dietary fiber, minerals and vitamins (Osorno et al., 2020), and also on. In addition, a recent study reported the presence of antioxidant compounds in kidney beans such as phenols and ketones (Yang et al., 2019), which have positive effects in managing diabetes, inhibiting obesity and increasing human metabolism (Liu, Zhang, et al., 2020; Neil et al., 2019; Nolan et al., 2020).

Although kidney beans are nutritious, it is hard to cook. This is because starch with high amylose content accounts for approximately 32% of the bean weight (Du, Jiang, Ai, & Jane, 2014; Gani et al., 2016; Liu, Peng, Zhang, Zou, & Zhong, 2013). The hydrogen bonds among these starch molecules make the bean very compact and a large amount of energy is required to destroy this structure during cooking (Du et al., 2014; Wani, Sogi, Wani, Gill, & Shivhare, 2010). Additionally, partially

cooked kidney beans can be toxic (Sun et al., 2020) due to the presence of naturally occurring toxin phytohemagglutinin. The consumption of partially cooked kidney beans can lead to food poisoning, including gastroenteritis, nausea, and diarrhea (Kumar, Verma, Das, Jain, & Dwivedi, 2013). The degradation of phytohemagglutinin is hindered by the compact structure of the kidney bean, too. Therefore, the raw kidney bean is not favored by the consumers with accelerating pace of life and the food industry to develop food products to target these consumers (Parmar, Singh, Kaur, & Thakur, 2017). To tackle this issue, there is an increasing demand to develop an efficient method to pre-gelatinize the kidney bean to improve its cooking efficiency.

To date, various drying techniques such as hot air and microwave drying have been used to pre-gelatinize kidney beans. Briefly, the hot air drying (HD) process can be used to remove the free moisture from the beans, as well as gelatinizing starch on their surface region (Ju et al., 2015). The HD process is not only easy to operate, but also low in manufacturing cost. High energy consumption and long drying time are the main factors limiting the development of HD process (Li, Liu, Gao, Xie, & Wang, 2021). On the other hand, the microwave radiation in the

---

* Corresponding author.
  E-mail address: lvweiqiao@cau.edu.cn (W. Lv).

microwave drying (MD) process heats both surface and interior regions of the food at the same time. This facilitates moisture migration and starch gelatinization during drying. Therefore, compared with the conventional drying method, microwave drying technique has the superiority of high drying efficiency and low energy consumption (Haghi & Amanifard, 2008). However, the major disadvantage of MD process is uneven drying of food products and it can cause the local carbonization of the kidney beans (Guo, Sun, Cheng, & Han, 2017; Li, Wang, & Kudra, 2011). Recently, microwave hot-air flow rolling drying (MARD) has been reported as a novel drying technique to combine the advantages of HD and MD techniques while minimizing the uneven drying of the food product (Su, Lv, Wang, Li, & Wang, 2020).

To the best of our knowledge, there is still a research paucity in investigating the pre-gelatinization of kidney beans using MHRD

technique. Therefore, in this study, we planned to investigate the drying kinetics of kidney beans dehydrated by both HD and MHRD techniques, as well as the effect of hot air temperature and microwave radiation on the characteristics of pre-gelatinized kidney beans in terms of microstructure, crystal structure and thermal properties. The texture profile of cooked pre-gelatinized kidney beans was also analyzed to explore its application. The outcome of this study is of great significance for the development of novel legume-based food products.

2. Materials and methods

2.1. Materials and pretreatment

Kidney beans (*Phaseolus vulgaris* L.) from mature flowered kidney
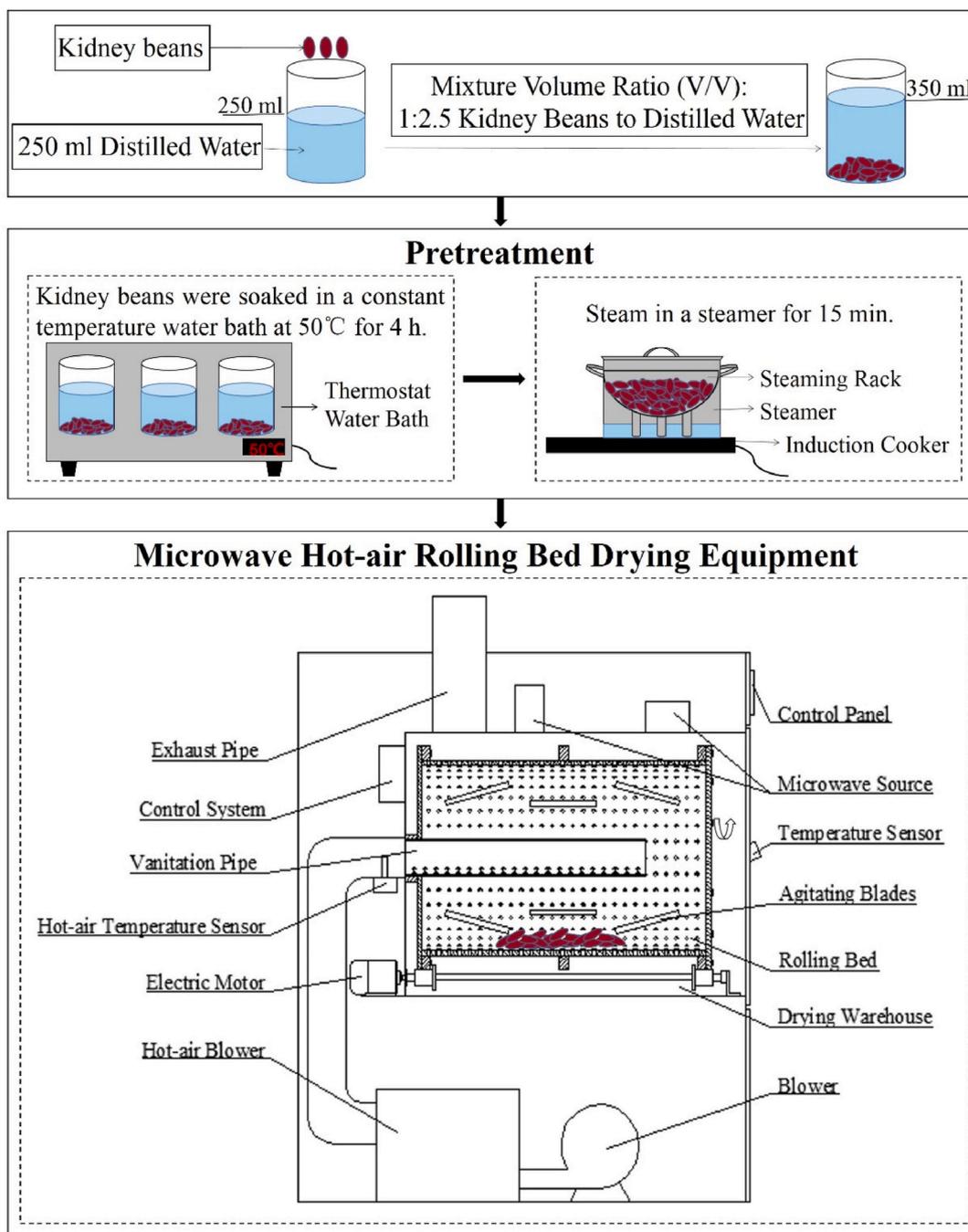

Fig. 1. Flow diagram of the whole process of drying kidney beans by microwave hot air rolling bed drying (MHRD) equipment.

beans, were purchased at the local agricultural market. All the beans were from the same batch and were free of pests and mechanical damage.

Before drying, the kidney beans were processed using the pretreatment protocol shown in Fig. 1. Briefly, the selected kidney beans were soaked in the water with a bean-to-water ratio of 1:2.5 (ml/ml) at 50 °C for 4 h. After the water on their surface was removed using absorbent paper, the beans were steamed for 15 min using a pot. After the steamed kidney beans were cooled to room temperature, the water on the bean surface was removed. The moisture content of these pretreated beans was obtained and dried at 105 °C using an oven until the weight did not change. And the moisture content of pretreated beans was 0.974 ± 0.003 g water/g solid (dry basis) (Li, Li, et al., 2021).

2.2. Drying equipment

The drying equipment used in the experiment is the ORW2S-3000R microwave hot air rolling bed dryer, which was jointly developed by the College of Engineering of China Agricultural University and Nanjing Aorun Company (Nanjing, Jiangsu, China). Its specific structure diagram is shown in Fig. 1. Briefly, the dryer is composed of a microwave system, hot air system, control system and rolling bed. The oven is a resonant cavity made of stainless steel with the size of 650 × 500 × 500 mm. The microwave system includes two independently controlled 2450 MHz microwave magnetrons on the top of the resonant cavity and the power of each can be adjustable in the range of 100–1000 W. The power of the hot air system is 3000 W and the temperature can be controlled from 20 to 180 °C, with an adjustable hot air speed from 0.1 to 2 m/s.

A control panel was installed on the drying chamber door to control the microwave power, drying time, rolling bed speed, and wind speed. The real-time surface temperature of the material can be monitored by an infrared temperature sensor. If the surface temperature of the material exceeds the allowed temperature, the microwave magnetrons stop working. The rotation speed of the drum can be controlled from 1 to 10 rpm, and the drum and the ventilation pipe are designed with air circulation holes to dry the materials (Su, Lv, Wang, Wang, & Li, 2020).

2.3. Drying of pre-treated kidney beans

The pretreated beans were brought to room temperature and the hot air blower was turned on for at least 5 min started to stabilize the airflow and temperature before they were dried using HD and MHRD techniques, respectively. For the HD process, pretreated beans were dried using the hot air with the temperature of 60–80 °C. During drying, the speed of hot air and drum was controlled at 0.5 m/s and 5 rpm, respectively. On the other hand, for the MHRD process, 600 g pretreated kidney beans were located in the drum and the rotation speed of the drum was set as 5 rpm. The microwave power was set to 0.8 W/g and the hot air temperature was set to 60–80 °C. In both HD and MHRD drying processes, the weight of the sample was measured every 30 and 10 min, respectively using an electronic balance with a sensitivity of 0.1 g. Once the moisture content of the beans was below 8% (wet basis), the drying was completed.

2.4. Drying kinetics of pre-treated kidney beans

The moisture ratio (MR) of pre-treated kidney beans during the drying process was calculated with the following Eq. (1):

$$MR = \frac{M_t - M_e}{M_o - M_e} \tag{1}$$

where MR is the moisture ratio, M_t (g water/g solid) represents the moisture content (dry basis) of the sample at any time, M_e represents the equilibrium moisture content and M_o represents the initial moisture

content (dry basis) of the sample. Because M_e is negligible compared with M_t and M_o, Eq. (1) can be further simplified into Eq. (2):

$$MR = \frac{M_t}{M_o} \tag{2}$$

The drying rate (DR, g/(g.min)) can be calculated with the following Eq. (3):

$$DR = \frac{M_{t1} - M_{t2}}{t_2 - t_1} \tag{3}$$

where M_{t1}, M_{t2} represent the moisture content (dry basis) of the sample at time t_1 and t_2, respectively.

2.5. Color profile

To study the effect of drying process on the color change of the kidney beans, the hulls of the dried kidney beans were removed and the color profile of the beans was characterized using a colorimeter (WF-10, Shenzhen Weifu Optoelectronics Technology Co., Ltd., China). Three color indices (L^* for brightness, a^* for redness and b^* for yellowness) were reported and a total color change (ΔE) was calculated with the following Eq. (4) (Aral & Bese, 2016) :

$$\Delta E = \sqrt{\left(L^* - L_0^*\right)^2 + \left(a^* - a_0^*\right)^2 + \left(b^* - b_0^*\right)^2} \tag{4}$$

where $L_0^*, a_0^*, b_0^*, L^*, a^*, b^*$ are the color index of pretreated and dried beans, respectively and $L_0^* = 61.31 \pm 0.27$, $a_0^* = 5.10 \pm 0.06$ and $b_0^* = 23.06 \pm 0.65$.

2.6. Extraction of kidney bean starch

Kidney bean starch was extracted from kidney beans using Wang et al. (Wang et al., 2021)'s method. Untreated and dried kidney beans were ground by a grinder, and the powder was sieved using a 100-mesh sieve. An approximate 50 g ground kidney bean flour was mixed with 200 g NaOH (0.2%, g/g) and the mixture was heated using a shaking water bath (SHZ-88A, Suzhou, China) at 37 °C and 120 rad/min for 6 h. The mixture was then centrifuged at 4000 r/min for 30 min (GL-20G-II, Shanghai, China). The upper layer of pigment was carefully removed and discarded. Subsequently, the precipitate was dispersed in distilled water and this mixture was centrifuged at 4000 r/min for 10 min to wash the precipitate. The washed precipitate was then dispersed in distilled water again and the mixture was neutralized using HCl (0.3%, g/g). After another centrifugation at 4000 r/min for 10 min, the precipitated kidney bean paste was collected and dried at 40 °C for 24 h using an oven. Finally, this dried kidney bean starch was passed through a 100-mesh sieve and stored at 4 °C before further use.

2.7. Morphology of kidney bean starch granule

A scanning electron microscope (SEM, SU3500; Hitachi Co., Tokyo, Japan) was used to observe the morphological characteristics of starch granules extracted from untreated and dried kidney beans, using Awais et al. (Awais et al., 2020)'s method. Briefly, the starch samples were evenly sprinkled on the conductive tape. After removing the excessive starch, the sample was coated with gold using a sputtering apparatus for 1 min. During the SEM imaging, the morphology of all the samples was observed at an accelerating voltage of 5.0 kV and the images were captured under 500× magnification.

2.8. Crystalline properties of kidney bean starch

The crystalline properties of the extracted kidney bean starch were studied using an X-ray diffractometer (XRD) (XD-2, Beijing Purkinje General Instrument Co., Ltd., China) using Li et al. (Li, Yan, et al.,

2021)'s method. Briefly, a Cu-Kα anode was used to generate radiation at 6 kV and 20 mA. The sample was scanned in the range of 4 to 40° (2θ) at the speed of 2°/min and 0.02 steps. The XDR spectra of the samples was recorded by MDI Jade 6 software to calculate their relative crystallinity. Origin 2018 software (Origin Lab, USA) was used to plot the X-ray diffraction data.

2.9. Thermal properties of kidney bean starch

The thermal properties of kidney bean starch were measured using a differential scanning calorimetry (DSC) (AR-2000ex, TA Instruments Ltd., New Castle, USA), using Ji et al. (Ji, Yu, Xu, & Zhang, 2016)'s method with minor modification. Briefly, 3 mg ± 0.1 mg kidney bean starch was accurately weighed into an aluminium pan. Subsequently, distilled water was added into the pan at a starch-to-water ratio of 1:3 (mg/mg). Then the pan was sealed and stored at room temperature for 12 h. For thermal property analysis, the stored sample was loaded in the vessel and heated from 30 to 120 °C at a rate of 10 °C/min. The thermogram of the kidney bean starch was recorded and gelatinization enthalpy change (ΔH), gelatinization range (ΔT) and initial (T_o), peak (T_p) and termination (T_c) temperatures were calculated by TA universal analysis 2000 software (4.5A, TA Instruments Ltd., USA). According to Li et al. (Li, Yan, et al., 2021)'s method, The degree of gelatinization of kidney bean starch (DG) can be calculated using the enthalpy value of gelatinized starch (ΔH_{par}) and the enthalpy value of natural starch (ΔH_{native}), as shown in Eq. (5):

$$DG = \left(1 - \Delta H_{par} / \Delta H_{native}\right) \times 100\% \tag{5}$$

2.10. Fourier transform infrared spectrometer (FTIR)

The FTIR spectra of the extracted starch samples was recorded using a SPECTRUM 100 FTIR spectrometer (PkinElmer, USA). Briefly, starch and potassium bromide (KBr) granules were mixed at 1:100 (mg/mg) and the mixture was ground in an agate mortar. Subsequently, this mixed sample was compressed to form a transparent sheet by a vacuum compressor. Thirty-two scans were taken and the data was averaged in each run in the range of 4000–400 cm^{-1} at 4 cm^{-1} resolution. The spectral analysis was made using OMNIC 8.2 (Thermo Fisher Scientific Inc., USA). The spectra in the range of 1200–900 cm^{-1} was further deconvoluted and the absorbance ratio at 1047/1022 was calculated to indicate the orderliness of short-range molecules in the crystalline phase. The absorption bands at 1047 and 1022 cm^{-1} represent the crystal structure and the amorphous structure, respectively (Wang et al., 2021).

2.11. Texture profile analysis (TPA)

The untreated and dried kidney beans using different drying methods were mixed with distilled at neutral pH at the bean-to-water ratio of 1:4 (ml/ml), followed by the steaming in a boiling water bath for 15 min. The texture characteristics of these steamed kidney beans were then measured using a texture analyzer (XT plus, Stable Micro Systems, UK) equipped with a cylindrical P36R probe in the distance mode using Li et al. (Li, Yan, et al., 2021)'s method. Briefly, the sample was compressed twice to 70% of its original height to mimic the chewing movement of the human mouth twice (Caine, Aalhus, Best, Dugan, & Jeremiah, 2003). The TPA settings were as follows: pre-test speed of 0.5 mm/s; post-test speed of 0.5 mm/s; target mode distance of how much and trigger force of 0.1 N. Each sample was measured multiple times by texture.

2.12. Data analysis

All experiments results were expressed as mean value ± standard deviation (SD). The data was analyzed using SPSS software, version 22.0 (SPSS Inc., Chicago, IL, USA). A comparison of means was made by Duncan's test at 5% significance level ($p < 0.05$) using one-way analysis of variance (ANOVA).

3. Results and discussions

3.1. Drying characteristics

The moisture ratio (MR) of kidney beans during HD and MHRD process is shown in Fig. 2A. Overall, the MR of the beans decreased gradually with the increase of drying time. The increase of hot air temperature significantly decreased the drying time, too, regardless of the drying method used. Particularly, when the hot air temperature was increased by 10 °C, drying time was decreased by approximately 27% (Fig. 2A). This is because the temperature of the material surface increased with the increase of hot air temperature, resulting in accelerated moisture evaporation (Md Salim, Gariépy, & Raghavan, 2017). As shown in Fig. 2A, the MHRD process significantly reduced the drying time of the kidney bean, compared with the HD process (approximately 2.5 times less), when hot air with the same temperature was used. This is because in the MHRD process, both the sample surface and interior region were heated at the same time so moisture migration and evaporation were accelerated (Maftoonazad, Dehghani, & Ramaswamy, 2020).

Fig. 2B illustrates the correlation between the drying rate (g/(g.min)) and the moisture content of the kidney bean (g water/g solid) when they were dried using HD and MHRD methods. Generally, the drying rate of all the materials decreased with the decrease of the moisture content and the highest drying rate was observed in the initial stage of the drying. This is due to the removal of free water (Aral & Bese, 2016; Zhu & Shen, 2014).

In addition, the incorporation of microwave radiation significantly accelerated the drying of the beans. For instance, the drying rate of the sample in the MHRD process in the initial stage of drying was more than 3 times higher than the one observed in the HD process, when the hot air with the same temperature was used (Fig. 2B). In this stage, the temperature of the beans was relatively low and the microwave was absorbed by the food material and converted into heat, which resulted in large temperature and vapor pressure difference between the interior region and surface of the material. This facilitated the moisture migration from the interior region to the surface and finally led to faster drying. As the drying continued, once the temperature of the material was beyond the allowed maximum temperature in the late drying stage, the microwave power reduced. This function was found to be effective to avoid the carbonization of the material during the MHRD process, caused by high temperature of the interior region of the food due to high microwave power (Ma, Luo, et al., 2021).

3.2. Color profile

Fig. 3 shows the color indices of kidney beans dried by HD and MHRD at different drying conditions. Thermal treatment and subsequent drying significantly affected the color profile of the dried sample surface. In both HD- and MHRD-processed kidney beans, the L* value of the dried samples decreased significantly with the increase of hot air temperature ($p < 0.05$). On the contrary, the value of b* slightly increased while the a* did not change significantly ($p > 0.05$). Also, the total color difference value (ΔE) increased significantly ($p < 0.05$) with the increase of hot air temperature.

Particularly, in the MHRD-processed kidney beans, the incorporation of microwave radiation increased b* and decreased L* value, respectively while it did not affect a* value significantly ($p < 0.05$). This effect of microwave on color change of kidney bean in the MHRD process was found to be similar to the one observed during the drying of potato and pleurotus eryngii (Ma, Luo, et al., 2021; Su, Lv, Wang, Wang, & Li, 2020). Overall, the effect of hot air temperature and microwave radiation on the color change of the beans during drying might be via the
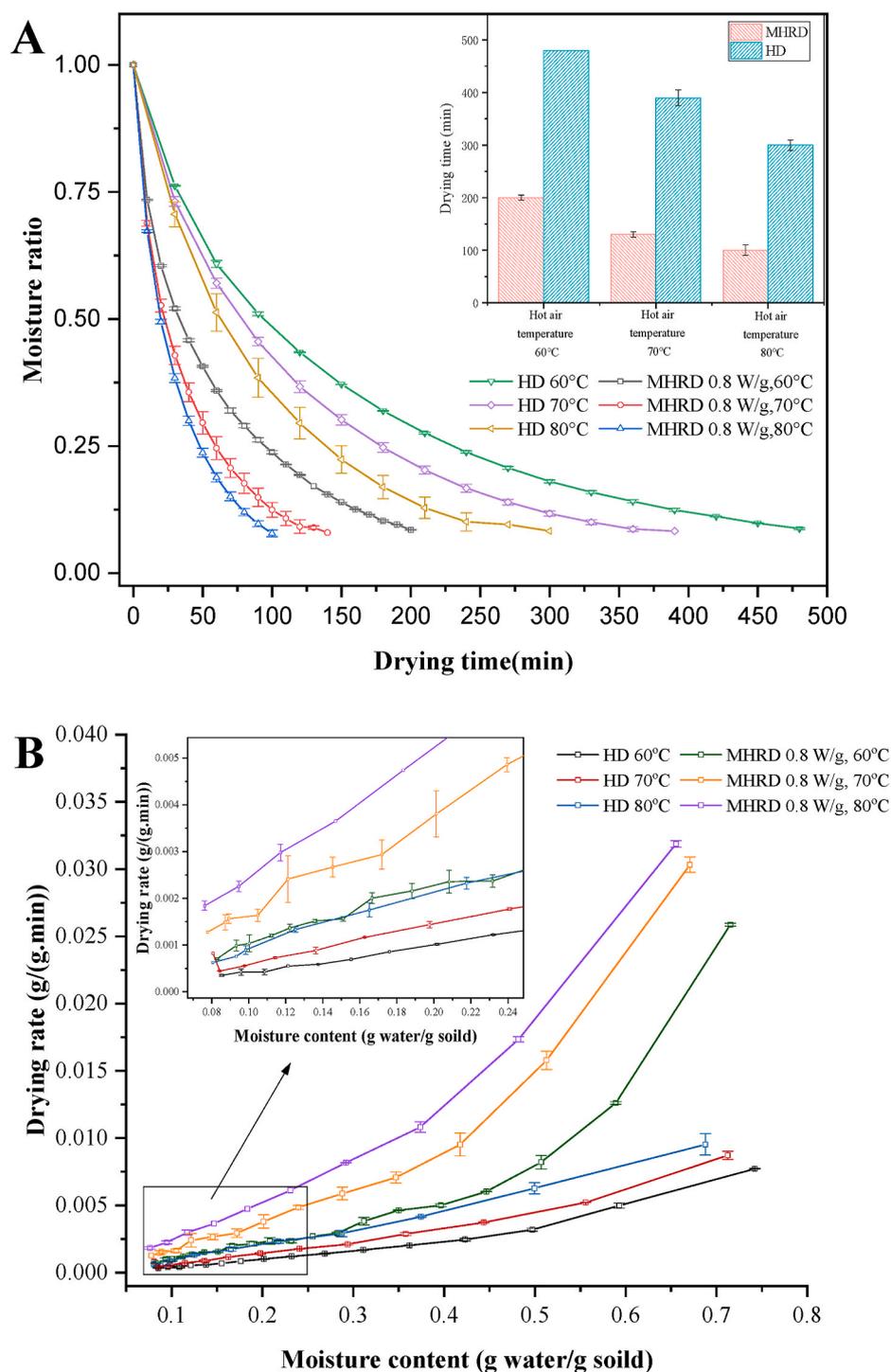
Fig. 2. Drying characteristic curves of kidney beans using different drying methods: A) Moisture content versus drying time; B) Drying rate versus moisture content.

occurrence of non-enzymatic browning reactions such as Maillard reaction (Jafari, Movagharnejad, & Sadeghi, 2020; Li, Wang, Wu, Wan, & Yang, 2020).

3.3. Morphology of kidney bean starch

The microstructure of the kidney bean starch is shown in Fig. 4. Untreated kidney bean starch exhibited an elliptical shape and smooth surface without cracks (Fig. 4A) (Bajaj, Singh, Kaur, & Inouchi, 2018). After pretreatment (soaking in water at 50 °C for 4 h and blanch for 15 min) and subsequent drying, the kidney bean starch had irregular rough

surfaces. This might be due to the starch agglomeration and gelatinization surrounding the granules. Due to the heat during drying, starch granules absorbed water and swelled to a certain extent until they were ruptured to leach the starch molecules (mainly amylose). These amylose molecules formed an interconnected network surrounding these granules via gelatinization. This starch agglomeration and gelatinization on the starch granules was also reported in the dried potato and rice starch (Ma, Xu, et al., 2021; Zhu et al., 2020).

After the pretreated kidney bean was dried using the HD method at the hot air temperature of 60 °C, some starch granules were connected to form large granule agglomerates. Meanwhile smaller individual
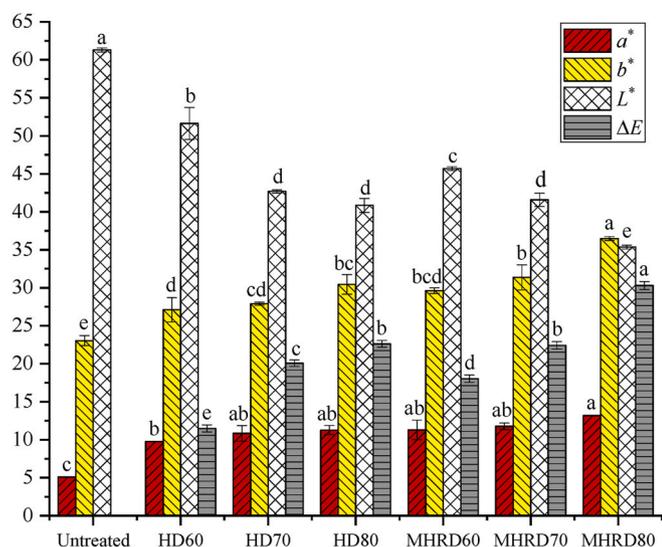
Fig. 3. Color indices of dehulled dried kidney beans obtained by different drying methods (Different letters above the bars indicate significant differences based on a Duncan test at a level of significance of $p < 0.05$). (For interpretation of the references to color in this figure legend, the reader is referred to the Web version of this article.)

granules still presented, with depressions on their rough surface (indicated by the arrows in Fig. 4B1). The size of these individual granules after drying exhibited a similar size with untreated kidney bean starch granules (Fig. 4A). However, with the increase of hot air temperature, these separated granules tended to interact with others to form large agglomerations (indicated by the arrows in Fig. 4B2-3). This is probably because more molecules were leached at the higher temperature,

resulting in an increased degree of starch gelatinization and finally it facilitate the agglomeration of starch granules. However, with the increase of hot air temperature, the inside of kidney beans absorbed more heat energy, and the degree of starch gelatinization also increased.

As shown in Fig. 4C1-3, in the MHRD-processed kidney beans, the starch granule agglomeration was more intensive, compared with HD-processed ones dried at the same hot air temperature. Particularly, few individual small starch granules were observed. This is due to the increased degree of starch gelatinization once microwave radiation was applied. Additionally, with the increase of hot air temperature, multiple starch granule agglomerates tended to interact and form a gel network (shown by the arrows in Fig. 4C2 and 3), indicating an even higher starch gelatinization degree. The change of kidney bean starch microstructure during drying in this study was similar to the one observed in mung bean and rice starch during their dehydration, respectively (Awais et al., 2020; Zhu et al., 2020).

3.4. Crystalline structure of kidney bean starch

The X-ray diffraction pattern of starch extracted from untreated and dried kidney beans is shown in Fig. 5A. Generally, the kidney bean starch had a typical A-type crystal structure and it exhibited strong diffraction peaks at 15, 17, 18 and 22.7°, respectively (Bajaj et al., 2018; Wang, Reddy, & Xu, 2018). The diffraction peaks of starch at 15° and 18° gradually disappeared with the increase of hot air temperature and the addition of microwave. The disappearance of the characteristic peak of A-type starch indicates that the crystal type of kidney bean starch changed and its original crystal structure was destroyed (Guo, Yu, Copeland, Wang, & Wang, 2018; Liu, Chen, Zheng, Xie, & Chen, 2020).

The relative crystallinity of starch extracted from untreated and dried beans was calculated and the result is shown in Table 1. Generally, the relative crystallinity suggests the orientation of the double helix in the crystal region of starch, the degree of interaction between the double
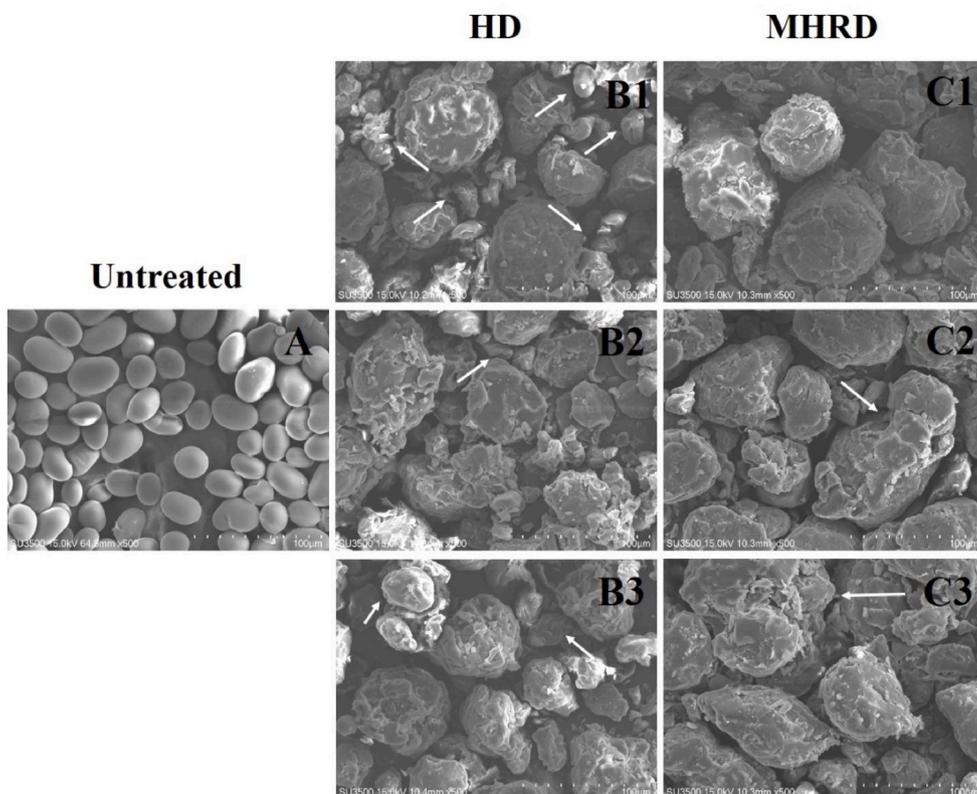

Fig. 4. SEM images of starch isolated from untreated and dried kidney beans: A) Untreated kidney bean starch; B1-3) Kidney bean starch from HD-60, 70 and 80, respectively and C1-3) Kidney bean starch from MHRD-60, 70 and 80 respectively (×500 magnification).
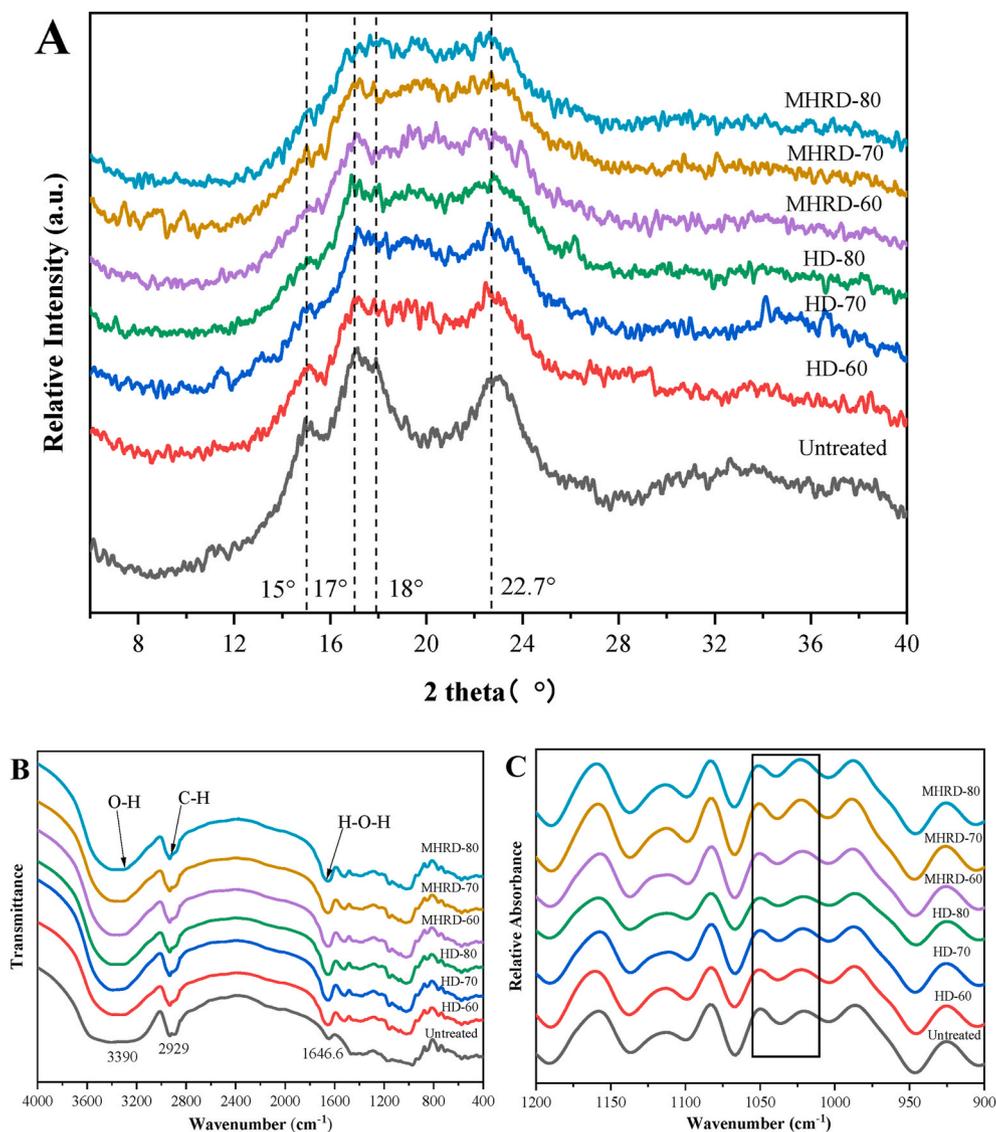
Fig. 5. XRD patterns and FTIR spectra of starch from untreated and dried kidney beans: A) XRD patterns; B) Original FTIR spectra in the range of 4000–400 cm^{-1} and C) Deconvoluted FTIR spectra in the range of 1200–900 cm^{-1}.

Table 1
DSC and XRD parameters of starch extracted from untreated and dried kidney beans using different drying methods.

Samples	T_o (°C)	T_p (°C)	T_c (°C)	ΔT (°C)	ΔH (J/g)	D.G. (%)	RC (%)
Untreated	63.62 ± 0.20[a]	71.48 ± 0.32[a]	81.72 ± 0.37[a]	18.10 ± 0.56[a]	12.17 ± 0.59[a]	ND	34.99 ± 0.60[a]
HD-60	60.63 ± 0.32[bc]	68.51 ± 0.28[c]	77.64 ± 0.73[b]	17.01 ± 0.75[bc]	3.106 ± 0.04[b]	74.48 ± 0.32[e]	32.38 ± 0.48[b]
HD-70	61.69 ± 0.94[b]	68.89 ± 0.17[bc]	76.52 ± 2.85[bc]	14.83 ± 2.18[c]	2.25 ± 0.01[c]	81.61 ± 0.15[d]	30.73 ± 0.34[c]
HD-80	61.73 ± 0.03[b]	69.42 ± 0.10[b]	75.70 ± 0.27[bc]	13.97 ± 0.29[c]	1.84 ± 0.12[cd]	84.90 ± 1.00[c]	29.18 ± 0.98[d]
MHRD-60	59.79 ± 0.69[c]	68.50 ± 0.01[c]	75.23 ± 0.29[bc]	15.43 ± 0.27[bc]	1.71 ± 0.03[cd]	85.98 ± 0.23[c]	29.47 ± 0.77[d]
MHRD-70	60.06 ± 0.77[c]	68.37 ± 0.33[c]	74.37 ± 0.40[c]	14.31 ± 0.34[c]	1.50 ± 0.08[de]	87.67 ± 0.63[b]	27.32 ± 0.19[e]
MHRD-80	59.70 ± 0.68[c]	66.85 ± 0.06[d]	71.28 ± 0.63[d]	11.58 ± 0.31[d]	0.97 ± 0.08[e]	92.05 ± 0.69[a]	25.72 ± 0.20[f]

Different letters above the bars indicate significant differences based on a Duncan test at a level of significance of $p < 0.05$.
T_o, initial gelatinization temperature; T_p, peak temperature; T_c, termination temperature; ΔT, gelatinization range; ΔH, enthalpy; DG, degree of gelatinization of kidney bean starch; RC, relative crystallinity.

strands and the number of long amylopectin chains (Hoover & Ratnayake, 2002). In both HD- or MHRD-processed kidney beans, the relative crystallinity (RC) of starch decreased significantly with the increase of hot air temperatures ($p < 0.05$). A similar trend was also reported in potato starch during heating (Liu, Chen, et al., 2020). This may be because the elevated temperature of the material during heating/-drying led to degradation of the starch crystallization area, partial

gelatinization of starch granules or destruction of the double helix structure, resulting in the destabilization of the crystal structure (Gou et al., 2019; Sun, Gong, Li, & Xiong, 2014). Compared with the starch extracted from HD-processed kidney beans, the one from MHRD-processed materials using hot air with the same temperature had significantly decreased diffraction intensity and the relative crystallinity (RC) ($p < 0.05$). This indicates more hydrogen bonds were destructed in

the MHRD-processed kidney bean starch than the one from HD-processed material. Therefore, the starch crystalline structure in the MHRD-processed kidney beans was more destabilized. It is because during the HD drying, only the starch on the surface of the kidney beans had a high degree of gelatinization while the gelatinization degree of the starch in the interior region remained low. However, in the MHRD process, both surface and interior region of the kidney bean were heated at the same time, leading to an increased transformation degree from ordered crystalline structure to disordered amorphous form (Cai et al., 2014).

3.5. Thermal properties

The gelatinization parameters of starch from untreated and dried kidney beans are presented in Table 1, in terms of initial gelatinization temperature (T_o), peak temperature (T_p) and termination temperature (T_c). Generally, a starch with more crystal structure has a higher gelatinization temperature. As shown in Table 1, the gelatinization temperature range (ΔT) of the starch from untreated beans was 63.62–81.72 °C and this agrees with the result reported by Hoover and Ratnayake (Hoover & Ratnayake, 2002). After thermal treatment and subsequent drying, the gelatinization temperature of kidney beans was significantly decreased ($p < 0.05$) and this trend was also observed in the starch extracted from dried mung beans (Awais et al., 2020). Additionally, the starch in the MHRD-processed kidney bean had a significantly lower gelatinization temperature than the one from HD-processed kidney beans, when the temperature of the hot air was the same ($p < 0.05$). This indicates more destruction occurred in the crystalline structure of the MHRD-processed beans. However, within the groups processed by HD or MHRD, the gelatinization temperature of kidney bean starch fluctuated in a relatively narrow range at different hot air temperatures. This might be caused due to the minor structural changes of the starch induced by different hot air temperatures (Wang et al., 2021).

The enthalpy (ΔH) represents the amount of energy that starch needs to absorb during its gelatinization and it is affected significantly by the crystallinity of starch (Liu, Liu, Fan, Qin, & Wang, 2020). When the temperature of hot air remained the same, the ΔH of starch in the MHRD-processed kidney bean was significantly lower than the one from HD-processed material ($p < 0.05$). Within HD- or MHRD-processed groups, the ΔH of starch decreased significantly ($p < 0.05$) with the increase of hot air temperature. These results are consistent with the changes in the relative crystallinity of the starch. As discussed in section 3.4, the MHRD process caused more destruction to the crystalline structure of kidney bean starch than the HD process so less energy was required for gelatinization (Lu et al., 2020). However, in the starch extracted from both HD- and MHRD-processed kidney beans, ΔH only varied in a narrow temperature range. The reason for this phenomenon may be that the effect of microwave energy on starch gelatinization was higher than that of hot air temperatures.

3.6. Fourier transform infrared spectroscopy (FTIR)

The FTIR spectra of starch extracted from untreated or dried kidney beans in the range of 4000–400 cm^{-1} is shown in Fig. 5B. Overall, the FTIR spectra of all the starch samples in dried kidney beans was found to be consistent with the one in the untreated sample, indicating no new chemical bonds were formed or the old chemical bonds disappeared during thermal treatment and subsequent drying (Awais et al., 2020; Wang, Zheng, & Tian, 2020). In Fig. 5B, the band at 3600-3000 cm^{-1} is caused by O–H stretching vibration. In the starch from dried beans, one can observe that the bandwidth of this O–H stretch decreased gradually with the increase of hot air temperature and incorporation of microwave radiation. Zhu et al. (2020) observed a similar trend during the heating of rice starch. The sharp bands at 2929 and 1646.6 cm^{-1} are due to asymmetric stretching of C–H and O–H–O bending vibration,

respectively (Sukhija, Singh, & Riar, 2016). The latter one is associated with the adsorbed water. Compared with the starch in the untreated beans, the one from dried beans exhibited increased peak intensity at 1646.6 cm^{-1}. This might be due to more water was absorbed by gelatinization during drying. A similar trend was observed during microwave-assisted esterification of starch (Lu et al., 2020).

The deconvolved FTIR spectra of kidney bean starch in the range of 1200–900 cm^{-1} is shown in Fig. 5C. The absorbance ratio of 1047/1022 of starch from untreated, HD-60, HD-70, HD-80, MHRD-60, MHRD-70, MHRD-80 were 1.015, 0.961, 0.936, 0.93, 0.918, 0.892 and 0.852, respectively. These absorbance ratio results further confirm the XRD result in section 3.4, i.e., the destruction of starch crystalline structure during heating and effect of hot air temperature and incorporation of microwave radiation on destabilizing starch crystalline structure. Similarly, Awais et al. (2020) and Ma, Xu, et al. (2021) reported the destruction of the hydrogen bonds in starch granules by heat energy, causing cleavage of double helix structure.

3.7. Texture profile analysis (TPA)

The texture profile of cooked untreated and dried kidney beans, in terms of hardness, springiness, gumminess and chewiness is shown in Fig. 6A–D, respectively. One can observe that the hardness, gumminess and chewiness of cooked untreated kidney beans were significantly higher than those of cooked dried ones ($p < 0.05$). This is due to the compact structure of untreated kidney beans, which compromises their water absorption ability during cooking. It finally resulted in incomplete starch gelatinization during cooking, i.e., these kidney beans were partially cooked (Rehman, Salariya, & Zafar, 2001). However, the pre-treatment and subsequently drying destroyed the crystalline structure of the kidney beans and gelatinized starch to a different extent (section 3.3 and 3.4), resulting in a relatively loose structure that was easier to be cooked. Meanwhile, the springiness of the dried kidney beans after cooking was significantly higher than the one of untreated beans ($p < 0.05$). The taste of pre-treated kidney beans after cooking may be better than that of untreated kidney beans. In addition, hot air temperature did not effect on the springiness of kidney beans after cooking significantly (Fig. 6B), while the effect of microwave was more significant.

As shown in Fig. 6A, C and D, the hardness, gumminess and chewiness of the dried kidney beans after cooking significantly decreased 1) with the increase of hot air temperature in the HD-process group or 2) with the incorporation of microwave radiation in the MHRD-process group, respectively (both $p < 0.05$). This is because more destabilized crystalline structure of the kidney beans was destabilized by the hot air at a higher temperature or upon microwave radiation. Similar results were observed during the gelatinization of rice grain, reported by Li, Yan, et al. (2021).

Among the cooked MHRD-processed kidney beans, one can observe the significant change in the hardness, springiness, gumminess and chewiness until the temperature of hot air exceeded 70 °C ($p < 0.05$). Therefore, based on the discussion in the above sections, thermal treatment followed by drying using the MHRD technique at the microwave power of 0.8 W/g and hot air temperature of 70 °C was considered to be the optimum processing method to produce pre-gelatinized kidney bean.

4. Conclusion

In this study, a novel process was developed to produce pre-gelatinized kidney beans using thermal treatment followed by the drying method. After soaking for 4 h and steaming for 15 min, the kidney beans were dried using HD or MHRD methods. The results showed that the increase of hot air temperatures and use of microwave radiation significantly improved drying efficiency. The microstructure, crystal structure, gelatinization characteristics and short-range molecular orderliness of kidney bean starch were further studied. The result
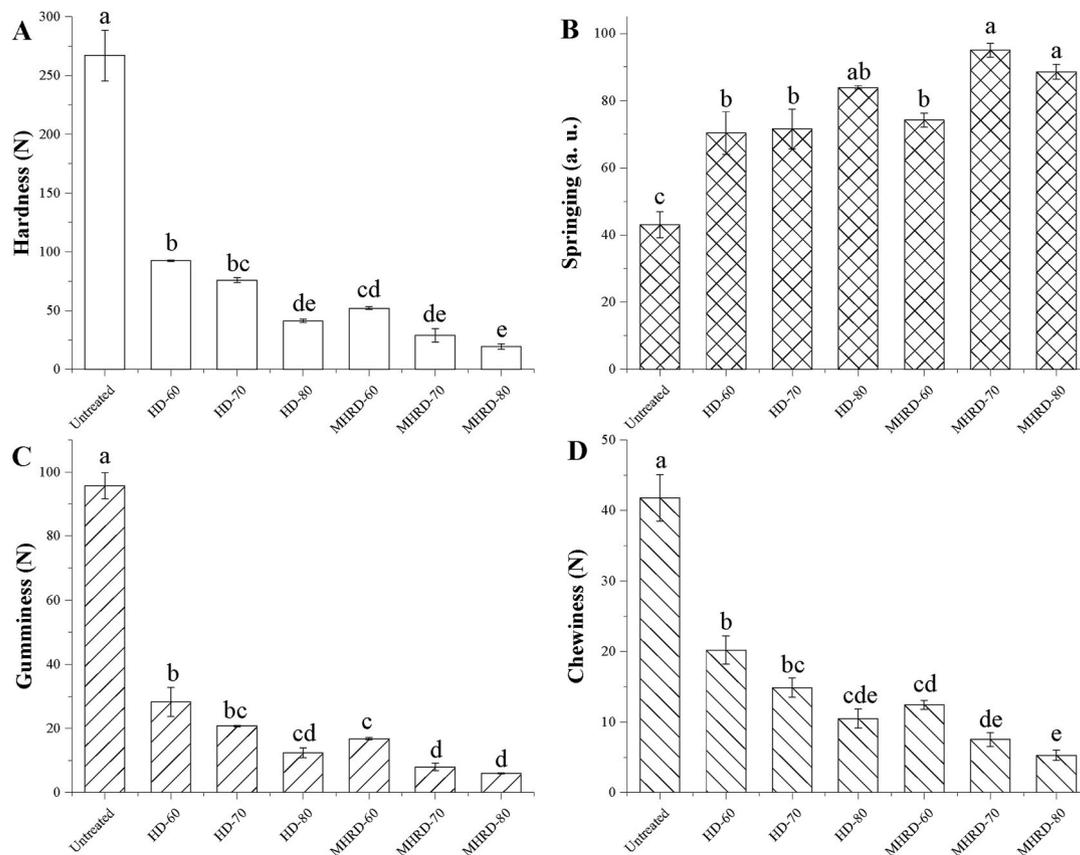
Fig. 6. Texture profile (TPA) of cooked untreated and dried kidney beans: A) Hardness (N); B) Springiness (a. u.); C) Gumminess (N) and D) Chewiness (N). Different letters above the bars indicate significant differences based on a Duncan test at a level of significance of $p < 0.05$.

suggested the positive correlation between hot air temperature/incorporation of microwave radiation and the destabilization of starch crystalline structure, as well as their gelatinization degree. Subsequently, the textural profile of the cooked dried kidney beans was studied, with the cooked untreated ones as control. The result indicated the dried beans could be completed cooked in a relatively short time. Overall, soaking for 4 h and steaming for 15 min, followed by MHRD drying at a microwave powder of 0.8 W/g and hot air temperature of 70 °C was found to be the optimum processing conditions to produce the dried kidney bean and this may provide industry researchers with useful insights for the development of food products.

CRediT authorship contribution statement

Mengge Li: Conceptualization, Methodology, Data curation, Writing – original draft, Investigation, Software, Formal analysis. **Bo Wang:** Formal analysis, Validation, Writing – review & editing. **Weiqiao Lv:** Resources, Validation, Funding acquisition, Project administration. **Rongru Lin:** Data curation, Writing – original draft, Investigation. **Donglin Zhao:** Visualization, Supervision, All authors read and approved the manuscript.

Declaration of competing interest

None.

Acknowledgements

References

Ahmed, J., Al-Ruwaih, N., Mulla, M., & Rahman, M. H. (2018). Effect of high pressure treatment on functional, rheological and structural properties of kidney bean protein isolate. *Lebensmittel-Wissenschaft und -Technologie- Food Science and Technology, 91*, 191–197. https://doi.org/10.1016/j.lwt.2018.01.054

Aral, S., & Bese, A. V. (2016). Convective drying of hawthorn fruit (Crataegus spp.): Effect of experimental parameters on drying kinetics, color, shrinkage, and rehydration capacity. *Food Chemistry, 210*, 577–584. https://doi.org/10.1016/j.foodchem.2016.04.128

Awais, M., Ashraf, J., Wang, L., Liu, L., Yang, X., Tong, L. T., et al. (2020). Effect of controlled hydrothermal treatments on mung bean starch structure and its relationship with digestibility. *Foods, 9*(5), 664. https://doi.org/10.3390/foods9050664

Bajaj, R., Singh, N., Kaur, A., & Inouchi, N. (2018). Structural, morphological, functional and digestibility properties of starches from cereals, tubers and legumes: A comparative study. *Journal of Food Science & Technology, 55*(9), 3799–3808. https://doi.org/10.1007/s13197-018-3342-4

Cai, C., Cai, J., Man, J., Yang, Y., Wang, Z., & Wei, C. (2014). Allomorph distribution and granule structure of lotus rhizome C-type starch during gelatinization. *Food Chemistry, 142*, 408–415. https://doi.org/10.1016/j.foodchem.2013.07.091

Caine, W. R., Aalhus, J. L., Best, D. R., Dugan, M. E. R., & Jeremiah, L. E. (2003). Relationship of texture profile analysis and Warner-Bratzler shear force with sensory characteristics of beef rib steaks. *Meat Science, 64*(4), 333–339. https://doi.org/10.1016/s0309-1740(02)00110-9

Du, S. K., Jiang, H., Ai, Y., & Jane, J. L. (2014). Physicochemical properties and digestibility of common bean (Phaseolus vulgaris L.) starches. *Carbohydrate Polymers, 108*, 200–205. https://doi.org/10.1016/j.carbpol.2014.03.004

Gani, A., Jan, A., Shah, A., Masoodi, F. A., Ahmad, M., Ashwar, B. A., et al. (2016). Physico-chemical, functional and structural properties of RS3/RS4 from kidney bean (Phaseolus vulgaris) cultivars. *International Journal of Biological Macromolecules, 87*, 514–521. https://doi.org/10.1016/j.ijbiomac.2016.03.017

Gou, M., Wu, H., Saleh, A. S. M., Jing, L., Liu, Y., Zhao, K., et al. (2019). Effects of repeated and continuous dry heat treatments on properties of sweet potato starch. *International Journal of Biological Macromolecules, 129*, 869–877. https://doi.org/10.1016/j.ijbiomac.2019.01.225

Guo, Q., Sun, D.-W., Cheng, J.-H., & Han, Z. (2017). Microwave processing techniques and their recent applications in the food industry. *Trends in Food Science & Technology, 67*, 236–247. https://doi.org/10.1016/j.tifs.2017.07.007

Guo, P., Yu, J., Copeland, L., Wang, S., & Wang, S. (2018). Mechanisms of starch gelatinization during heating of wheat flour and its effect on in vitro starch digestibility. *Food Hydrocolloids, 82*, 370–378. https://doi.org/10.1016/j.foodhyd.2018.04.012

Haghi, A. K., & Amanifard, N. (2008). Analysis of heat and mass transfer during microwave drying of food products. *Brazilian Journal of Chemical Engineering, 25*(3), 491–501. https://doi.org/10.1590/S0104-66322008000300007

Hoover, R., & Ratnayake, W. S. (2002). Starch characteristics of black bean, chickpea, lentil, navy bean and pinto bean cultivars grown in Canada. *Food Chemistry, 78*(4), 489–498. https://doi.org/10.1016/S0308-8146(02)00163-2

Jafari, F., Movagharnejad, K., & Sadeghi, E. (2020). Infrared drying effects on the quality of eggplant slices and process optimization using response surface methodology. *Food Chemistry, 333*, 127423. https://doi.org/10.1016/j.foodchem.2020.127423

Ji, Y., Yu, J., Xu, Y., & Zhang, Y. (2016). Impact of dry heating on physicochemical properties of corn starch and lysine mixture. *International Journal of Biological Macromolecules, 91*, 872–876. https://doi.org/10.1016/j.ijbiomac.2016.06.040

Ju, H.-Y., El-Mashad, H. M., Fang, X.-M., Pan, Z., Xiao, H.-W., Liu, Y.-H., et al. (2015). Drying characteristics and modeling of yam slices under different relative humidity conditions. *Drying Technology, 34*(3), 296–306. https://doi.org/10.1080/07373937.2015.1052082

Kumar, S., Verma, A. K., Das, M., Jain, S. K., & Dwivedi, P. D. (2013). Clinical complications of kidney bean (Phaseolus vulgaris L.) consumption. *Nutrition, 29*(6), 821–827. https://doi.org/10.1016/j.nut.2012.11.010

Li, J., Li, Z., Li, L., Song, C., Raghavan, G. S. V., & He, F. (2021b). Microwave drying of balsam pear with online aroma detection and control. *Journal of Food Engineering, 288*, 110139. https://doi.org/10.1016/j.jfoodeng.2020.110139

Li, X., Liu, Y., Gao, Z., Xie, Y., & Wang, H. (2021). Computer vision online measurement of shiitake mushroom (Lentinus edodes) surface wrinkling and shrinkage during hot air drying with humidity control. *Journal of Food Engineering, 292*, 110253. https://doi.org/10.1016/j.jfoodeng.2020.110253

Liu, Z., Chen, H., Zheng, B., Xie, F., & Chen, L. (2020b). Understanding the structure and rheological properties of potato starch induced by hot-extrusion 3D printing. *Food Hydrocolloids, 105*, 105812. https://doi.org/10.1016/j.foodhyd.2020.105812

Liu, X. X., Liu, H. M., Fan, L. Y., Qin, G. Y., & Wang, X. D. (2020). Effect of various drying pretreatments on the structural and functional properties of starch isolated from Chinese yam (Dioscorea opposita Thumb.). *International Journal of Biological Macromolecules, 153*, 1299–1309. https://doi.org/10.1016/j.ijbiomac.2019.10.265

Liu, B., Peng, J., Zhang, S., Zou, B., & Zhong, G. (2013). Chemical composition,in vitrostarch digestibility and amino acid analysis of a underexplored kidney bean (Phaseolus vulgaris. L.) grown in Chongqing, China. *International Journal of Food Science and Technology, 48*(3), 527–532. https://doi.org/10.1111/j.1365-2621.2012.03214.x

Liu, Y., Zhang, J., Guo, H., Zhao, A., Shao, D., Dong, Z., et al. (2020a). Effects of mulberry leaf and white kidney bean extract mix on postprandial glycaemic control in pre-diabetic subjects aged 45–65 years: A randomized controlled trial. *Journal of Functional Foods, 73*, 104117. https://doi.org/10.1016/j.jff.2020.104117

Li, Z. Y., Wang, R. F., & Kudra, T. (2011). Uniformity issue in microwave drying. *Drying Technology, 29*(6), 652–660. https://doi.org/10.1080/07373937.2010.521963

Li, Y., Wang, X., Wu, Z., Wan, N., & Yang, M. (2020). Dehydration of hawthorn fruit juices using ultrasound-assisted vacuum drying. *Ultrasonics Sonochemistry, 68*, 105219. https://doi.org/10.1016/j.ultsonch.2020.105219

Li, H., Yan, S., Yang, L., Xu, M., Ji, J., Mao, H., et al. (2021a). Starch gelatinization in the surface layer of rice grains is crucial in reducing the stickiness of parboiled rice. *Food Chemistry, 341*, 128202. https://doi.org/10.1016/j.foodchem.2020.128202

Lu, K., Zhu, J., Bao, X., Liu, H., Yu, L., & Chen, L. (2020). Effect of starch microstructure on microwave-assisted esterification. *International Journal of Biological Macromolecules, 164*, 2550–2557. https://doi.org/10.1016/j.ijbiomac.2020.08.099

Maftoonazad, N., Dehghani, M. R., & Ramaswamy, H. S. (2020). Hybrid microwave-hot air tunnel drying of onion slices: Drying kinetics, energy efficiency, product rehydration, color, and flavor characteristics. *Drying Technology*, 1–21. https://doi.org/10.1080/07373937.2020.1841790

Ma, X., Luo, G., Li, Z., Raghavan, G. S. V., Chen, H., & Song, C. (2021a). Microwave power control scheme for potatoes based on dielectric loss factor feedback. *Journal of Food Engineering, 288*, 110134. https://doi.org/10.1016/j.jfoodeng.2020.110134

Ma, Y., Xu, D., Sang, S., Jin, Y., Xu, X., & Cui, B. (2021b). Effect of superheated steam treatment on the structural and digestible properties of wheat flour. *Food Hydrocolloids, 112*, 106362. https://doi.org/10.1016/j.foodhyd.2020.106362

Md Salim, N. S., Gariépy, Y., & Raghavan, V. (2017). Hot air drying and microwave-assisted hot air drying of broccoli stalk slices (Brassica oleracea L. Var. Italica). *Journal of Food Processing and Preservation, 41*(3), Article e12905. https://doi.org/10.1111/jfpp.12905

Neil, E. S., McGinley, J. N., Fitzgerald, V. K., Lauck, C. A., Tabke, J. A., Streeter-McDonald, M. R., et al. (2019). White kidney bean (Phaseolus vulgaris L.) consumption reduces fat accumulation in a polygenic mouse model of obesity. *Nutrients, 11*(11), 2780. https://doi.org/10.3390/nu11112780

Nolan, R., Shannon, O. M., Robinson, N., Joel, A., Houghton, D., & Malcomson, F. C. (2020). It's No has bean: A review of the effects of white kidney bean extract on body composition and metabolic health. *Nutrients, 12*(5), 1398. https://doi.org/10.3390/nu12051398

Osorno, J. M., Vander Wal, A. J., Posch, J., Simons, K., Grafton, K. F., & Pasche, J. S. (2020). 'ND Whitetail', a new white kidney bean with high seed yield and intermediate resistance to white mold and bacterial blights. *Journal of Plant Registrations, 14*(2), 102–109. https://doi.org/10.1002/plr2.20012

Parmar, N., Singh, N., Kaur, A., & Thakur, S. (2017). Comparison of color, anti-nutritional factors, minerals, phenolic profile and protein digestibility between hard-to-cook and easy-to-cook grains from different kidney bean (Phaseolus vulgaris) accessions. *Journal of Food Science & Technology, 54*(4), 1023–1034. https://doi.org/10.1007/s13197-017-2538-3

Punia, S., Dhull, S. B., Sandhu, K. S., Kaur, M., & Purewal, S. S. (2020). Kidney bean (Phaseolus vulgaris) starch: A review. *Legume Science, 2*(3), e52. https://doi.org/10.1002/leg3.52

Qin, G., Wang, F., Liang, H., Tang, S., Shekh, K., Wang, Y., et al. (2019). Subchronic study of a white kidney bean (Phaseolus vulgaris) extract with alpha-amylase inhibitory activity. *BioMed Research International*, 9272345. https://doi.org/10.1155/2019/9272345, 2019.

Rehman, Z., Salariya, A., & Zafar, S. (2001). Effect of processing on available carbohydrate content and starch digestibility of kidney beans (Phaseolus vulgaris L.). *Food Chemistry, 73*(3), 351–355. https://doi.org/10.1016/S0308-8146(00)00311-3

Sukhija, S., Singh, S., & Riar, C. S. (2016). Effect of oxidation, cross-linking and dual modification on physicochemical, crystallinity, morphological, pasting and thermal characteristics of elephant foot yam (Amorphophallus paeoniifolius) starch. *Food Hydrocolloids, 55*, 56–64. https://doi.org/10.1016/j.foodhyd.2015.11.003

Su, D., Lv, W., Wang, Y., Li, D., & Wang, L. (2020a). Drying characteristics and water dynamics during microwave hot-air flow rolling drying of Pleurotus eryngii. *Drying Technology, 38*(11), 1493–1504. https://doi.org/10.1080/07373937.2019.1648291

Su, D., Lv, W., Wang, Y., Wang, L., & Li, D. (2020b). Influence of microwave hot-air flow rolling dry-blanching on microstructure, water migration and quality of pleurotus eryngii during hot-air drying. *Food Control, 114*, 107228. https://doi.org/10.1016/j.foodcont.2020.107228

Sun, Q., Gong, M., Li, Y., & Xiong, L. (2014). Effect of dry heat treatment on the physicochemical properties and structure of proso millet flour and starch. *Carbohydrate Polymers, 110*, 128–134. https://doi.org/10.1016/j.carbpol.2014.03.090

Sun, X., He, S., Ye, Y., Cao, X., Liu, H., Wu, Z., et al. (2020). Combined effects of pH and thermal treatments on IgE-binding capacity and conformational structures of lectin from black kidney bean (*Phaseolus vulgaris* L.). *Food Chemistry, 329*, 127183. https://doi.org/10.1016/j.foodchem.2020.127183

Wang, X., Reddy, C. K., & Xu, B. (2018). A systematic comparative study on morphological, crystallinity, pasting, thermal and functional characteristics of starches resources utilized in China. *Food Chemistry, 259*, 81–88. https://doi.org/10.1016/j.foodchem.2018.03.121

Wang, H., Xu, K., Liu, X., Zhang, Y., Xie, X., & Zhang, H. (2021). Understanding the structural, pasting and digestion properties of starch isolated from frozen wheat dough. *Food Hydrocolloids, 111*, 106168. https://doi.org/10.1016/j.foodhyd.2020.106168

Wang, W., Zheng, B., & Tian, Y. (2020). Functional group changes and chemical bond-dependent dielectric properties of lotus seed flour with microwave vacuum drying. *Journal of Food Science, 85*(12), 4241–4248. https://doi.org/10.1111/1750-3841.15492

Wani, I. A., Sogi, D. S., Wani, A. A., Gill, B. S., & Shivhare, U. S. (2010). Physico-chemical properties of starches from Indian kidney bean (Phaseolus vulgaris) cultivars. *International Journal of Food Science and Technology, 45*(10), 2176–2185. https://doi.org/10.1111/j.1365-2621.2010.02379.x

Yang, Q.-Q., Gan, R.-Y., Zhang, D., Ge, Y.-Y., Cheng, L.-Z., & Corke, H. (2019). Optimization of kidney bean antioxidants using RSM & ANN and characterization of antioxidant profile by UPLC-QTOF-MS. *Lebensmittel-Wissenschaft und -Technologie-Food Science and Technology, 114*, 108321. https://doi.org/10.1016/j.lwt.2019.108321

Zhu, A., & Shen, X. (2014). The model and mass transfer characteristics of convection drying of peach slices. *International Journal of Heat and Mass Transfer, 72*, 345–351. https://doi.org/10.1016/j.ijheatmasstransfer.2014.01.001

Zhu, P., Wang, M., Du, X., Chen, Z., Liu, C., & Hao, Z. (2020). Morphological and physicochemical properties of rice starch dry heated with whey protein isolate. *Food Hydrocolloids, 109*, 106091. https://doi.org/10.1016/j.foodhyd.2020.106091